

# FLUID FORCES ON ROTATING CENTRIFUGAL IMPELLER

## WITH WHIRLING MOTION\*

Hidenobu Shoji and Hideo Ohashi  
University of Tokyo  
Tokyo, Japan

### SUMMARY

Fluid forces on a centrifugal impeller, whose rotating axis whirls with a constant speed, have been calculated by using unsteady potential theory. To simplify the problem, it is assumed that the flow is incompressible and two dimensional, the impeller is surrounded by vaneless diffuser and the eccentricity is constant and small. Calculations are performed for various values of whirl speed, number of impeller blades and angle of blades. Some typical examples of results are shown in vector diagrams. Although the results of this paper are obtained for simplified geometries under idealized assumptions, they will suggest us the nature of fluid forces acting on whirling impeller.

### INTRODUCTION

Recent advances in rotor dynamics made it possible to analyse very complicated rotor system like multi-stage pump rotor and multi-bearing turbogenerator shafting. In these analyses the largest weakness seems still to lie in the assumption of radial fluid forces acting on rotor elements such as seal rings, balance pistons and impellers. Many studies have been made and are being carried on this subject; just to mention a few, contribution of Black to pressure seal and centrifugal impeller (ref. 1,2) and of Acosta to centrifugal impeller (ref. 3).

As to radial forces acting on centrifugal impellers, numerous studies and informations have been accumulated on their steady part caused mainly by asymmetric configuration of volute casings. To the contrary limited studies (ref. 2,3) have been published on the unsteady part of radial forces, which is caused by the whirling motion of rotating impeller. This is the very information sought for the improvement of rotor analysis. Most of them are, however, quasi-steady analyses, in which the effect of shed vortices is disregarded.

In this paper, the radial force of a rotating impeller with arbitrary whirling motion is reduced from the flow fields in and outside of the impeller, applying familiar singularity method for the calculation of unsteady potential flow. Though the flow in a real centrifugal turbomachine is very complex because of asymmetric geometry of casing and strong viscous effect in impeller passage for example, following simplifications and assumptions are introduced in the present theory.

---

\*Not presented at workshop.

- (1) The fluid is incompressible and inviscid, and the flow is two dimensional and irrotational in the absolute coordinate system.
- (2) The region outside of the rotor is unbounded and free of vanes.
- (3) The ratio of whirl eccentricity to the radius of the impeller is so small that its square can be neglected.
- (4) The flow rate, the prerotation of suction flow, the rotational speed of the impeller and the whirling speed of the shaft center are constant.
- (5) Blades of impeller have no thickness and have the shape of logarithmic spiral.
- (6) Steady part of the flow satisfies the condition of shockless entry at the leading edges of the blades and Kutta's condition at the trailing edges is assumed.
- (7) Free vortices are shed from the trailing edges and are carried downstream along steady streamlines with steady velocities.

After having derived formulations of radial forces for given parameters of whirl to rotational speed ratio, number of impeller vanes and blade angle, typical numerical results are demonstrated in vector diagrams.

#### SYMBOLS

N	number of blades	$\beta$	angle between radius and blades
$r_1$	inside radius of impeller	$r_2$	outside radius of impeller
$\omega$	angular speed of impeller, positive clockwise		
$\Omega$	angular speed of whirling motion, positive clockwise		
$\epsilon$	eccentric radius	Q	flow rate
$\Gamma_p$	prerotation	$\rho$	density of fluid
$\gamma$	strength of vortices	$\bar{z}$	complex conjugate of z
i	complex unit with respect to coordinate		
j	complex unit with respect to time		

#### Subscripts

n	component normal to blade	t	component tangential to blade
s	steady component	0	quasi-steady component
w	component caused by free vortices		
$\omega$	component caused by rotation effect		

## ANALYSIS

### Basic Consideration

The centrifugal impeller shown in figure 1 is considered. It rotates with a constant angular speed  $\omega$  and its center whirls with a constant eccentric radius  $\epsilon$  and a constant angular speed  $\Omega$ . The boundary condition to the velocity field is in this case unsteady, and the flow around the impeller should be determined by unsteady analysis.

Let an arbitrary point on a reference blade be A. Then the geometry of the points A, O and O' are shown in figure 2, where point O and O' are the center of impeller and whirling motion, respectively. From the viewpoint of flow field, we interpret that the inlet flow to the impeller is unaffected by the whirling motion of the impeller, that is, the location of source Q (representing flow rate) and circulation  $\Gamma_p$  (representing prerotation) is fixed on point O'. Defining the angles  $\beta$ ,  $\theta_1$  and  $\theta_2$  as shown in figure 2, and introducing the lengths  $AO'=\ell$ ,  $AO=r$  and  $OO'=\epsilon$ ,  $\ell$  is expressed as

$$\ell = [r^2 + 2 r \cos(\theta_2 - \theta_1) + \epsilon^2]^{1/2} = r [1 + \epsilon/r \cos(\theta_2 - \theta_1)]$$

The velocity  $v_Q$  at A induced by source Q in the direction of O'A is

$$v_Q = Q/2 \pi \ell \cong Q/2 \pi r [1 - \epsilon/r \cos(\theta_2 - \theta_1)] \quad (1)$$

Similarly, the velocity  $v_\Gamma$  at A induced by circulation  $\Gamma_p$  is

$$v_\Gamma \cong \Gamma_p/2 \pi r [1 - \epsilon/r \cos(\theta_2 - \theta_1)] \quad (2)$$

where its direction is normal to the line O'A (positive clockwise).

The velocities  $v_Q$  and  $v_\Gamma$  are divided into two components respectively. They are  $v_{Qn}$  and  $v_{\Gamma n}$  which are normal to blade, and  $v_{Qt}$  and  $v_{\Gamma t}$  which are tangential to blade. As the reference blade intersects the line OA at angle  $\beta$ , the intersection angle between blade and line O'A is given approximately by  $\beta + (\epsilon/r) \sin(\theta_2 - \theta_1)$ . Using the above relations,  $v_{Qn}$ ,  $v_{\Gamma n}$ ,  $v_{Qt}$  and  $v_{\Gamma t}$  can be expressed as

$$v_{Qn} \cong Q/2 \pi r [\sin \beta + \epsilon/r \sin(\theta_2 - \theta_1 - \beta)] \quad (3)$$

$$v_{\Gamma n} \cong \Gamma_p/2 \pi r [\cos \beta - \epsilon/r \cos(\theta_2 - \theta_1 - \beta)] \quad (4)$$

$$v_{Qt} \cong Q/2 \pi r [\cos \beta - \epsilon/r \cos(\theta_2 - \theta_1 - \beta)] \quad (5)$$

$$v_{\Gamma t} \cong - \Gamma_p/2 \pi r [\sin \beta + \epsilon/r \sin(\theta_2 - \theta_1 - \beta)] \quad (6)$$

When point A on the blade is observed from a fixed coordinate system, A is moving in the normal direction to OA with velocity  $r\omega$ , and also in the normal direction to OO' with velocity  $\epsilon\Omega$ . Both velocities are considered positive clockwise. On the other hand, when observed from the relative coordinate system fixed to the rotating impeller, absolutely still field is considered to have velocities  $-r\omega$  and  $-\epsilon\Omega$  in the corresponding directions. These are divided into two components in the same way as  $v_Q$  and  $v_\Gamma$ . Using the relations

$d\theta_1/dt = -\Omega$  and  $d\theta_2/dt = -\omega$ , normal and tangential components  $v_{\omega n}$  and  $v_{\omega t}$  are

$$v_{\omega n} = -r \omega \cos \beta - \epsilon \Omega \cos(\theta_2 - \theta_1 + \beta) \quad (7)$$

$$v_{\omega t} = r \omega \sin \beta + \epsilon \Omega \sin(\theta_2 - \theta_1 + \beta) \quad (8)$$

Hereafter only relative coordinate system fixed to the impeller will be used. Every vector quantity such as location vector OA, force and velocity is indicated in this coordinate system by a complex number, whose real and imaginary (with imaginary unit  $i$ ) part represents its component in two orthogonal axes.

Imaginary unit with respect to time,  $j$ , is also introduced to indicate the phase difference of oscillating quantities. Since two complex units  $i$  and  $j$  have completely different meanings, they should be distinguished carefully in the reduction of equations.

Let the location of A be  $z$  in the complex plane, normal component  $v_{Qn}$ ,  $v_{\Gamma n}$  and  $v_{\omega n}$  of equations (3), (5) and (7) can be written as

$$v_{Qn} = \frac{Q}{2\pi|z|} [\sin \beta + j \epsilon \frac{\bar{z}}{|z|^2} e^{j\beta} e^{j(\omega-\Omega)t}]_j = v_{Qn1} + v_{Qn2} \quad (9)$$

$$v_{\Gamma n} = \frac{\Gamma p}{2\pi|z|} [\cos \beta - \epsilon \frac{\bar{z}}{|z|^2} e^{j\beta} e^{j(\omega-\Omega)t}]_j = v_{\Gamma n1} + v_{\Gamma n2} \quad (10)$$

$$v_{\omega n} = [-|z|\omega \cos \beta - \epsilon \frac{\bar{z}}{|z|} \Omega e^{-j\beta} e^{j(\omega-\Omega)t}]_j = v_{\omega n1} + v_{\omega n2} \quad (11)$$

Since only absolute values of above three quantities are of interest, they are expressed as a complex with respect only to  $j$ . Further, tangential component  $v_{Qt}$ ,  $v_{\Gamma t}$  and  $v_{\omega t}$  of equations (4), (6) and (8) are written as

$$\begin{aligned} v_{Qt} &= \frac{Q}{2\pi|z|} [\cos \beta - \epsilon \frac{\bar{z}}{|z|^2} e^{j\beta} e^{j(\omega-\Omega)t}]_j \cdot [\frac{z}{|z|} e^{i\beta}]_i \\ &= v_{Qt1} + v_{Qt2} \end{aligned} \quad (12)$$

$$\begin{aligned} v_{\Gamma t} &= -\frac{\Gamma p}{2\pi|z|} [\sin \beta + j \epsilon \frac{\bar{z}}{|z|^2} e^{j\beta} e^{j(\omega-\Omega)t}]_j \cdot [\frac{z}{|z|} e^{i\beta}]_i \\ &= v_{\Gamma t1} + v_{\Gamma t2} \end{aligned} \quad (13)$$

$$\begin{aligned} v_{\omega t} &= [|z|\omega \sin \beta + \epsilon \Omega j \frac{\bar{z}}{|z|} e^{-j\beta} e^{j(\omega-\Omega)t}]_j \cdot [\frac{z}{|z|} e^{i\beta}]_i \\ &= v_{\omega t1} + v_{\omega t2} \end{aligned} \quad (14)$$

All of the equations from (9) to (14) consist of the steady term indicated by subscript 1, and the unsteady term by subscript 2. Unsteady components are first order quantities in comparison with the steady component.

Since all the unsteady terms contain  $e^{j(\omega-\Omega)t}$ , this problem can be thought to be the periodic phenomenon with angular speed  $(\omega-\Omega)$ . All quantities within [ ]<sub>j</sub> are complex with respect to j, and therefore their argument corresponds to the phase of sinusoidally oscillating phenomenon.

### Steady Flow

As thickness of blades is disregarded, blades can be replaced by the distribution of vortices. The distribution of steady vortices  $\gamma_s$  has to satisfy the boundary condition that there is no crossing flow through blades. This leads to

$$\int_{z_L}^{z_T} \gamma_s(z') \operatorname{Re} \left( \frac{N}{2\pi} \frac{z^N}{z^N - z'^N} \frac{e^{i\beta}}{|z|} \right) dz' + v_{Qn1} + v_{\Gamma n1} + v_{\omega n1} = 0 \quad (15)$$

where  $z_L$  and  $z_T$  are the complex coordinates at leading and trailing edges of the blade. The integral should be carried out along the blade. For the calculation of the integrand of the above integral, the following relation is also used

$$\sum_{k=1}^N \frac{1}{z - z' e^{i2\pi k/N}} = \frac{N z^{N-1}}{z^N - z'^N} \quad (16)$$

Combining equation (15) and the Kutta's condition at the trailing edge,  $\gamma_s$  can be determined. As shockless entry at the leading edge is assumed in this analysis,  $\gamma_s$  is restricted to finite value. Once  $\gamma_s$  is obtained, the velocity  $v(z)$  at an arbitrary point  $z$  can be calculated by

$$v(z) = \int_{z_L}^{z_T} \gamma_s(z') \frac{N}{2\pi} \left( \frac{z^{N-1}}{z^N - z'^N} \right) dz' + \frac{z(Q - i\Gamma_p)}{2\pi |z|^2} + i z \omega \quad (17)$$

### Unsteady Flow

First we consider the flow field shown in figure 3, in which  $N$  discrete vortices with phase difference  $2\pi/N$  are ranged on a circumference with equal distance. Let the location of a reference vortex be  $z'$ , the complex conjugate velocity at an arbitrary point  $z$  is given as

$$f(z, z') = u - i v = \frac{i}{2\pi} \frac{\Gamma}{\pi} \sum_{k=1}^N \frac{e^{-j2\pi k/N}}{z - z' e^{i2\pi k/N}}$$

$$= \frac{iN\Gamma}{4\pi z} \left[ \frac{(z/z')^{N/2-1} + (z'/z)^{N/2-1}}{(z/z')^{N/2} - (z'/z)^{N/2}} - i \frac{j(z/z')^{N/2-1} - (z'/z)^{N/2-1}}{(z/z')^{N/2} - (z'/z)^{N/2}} \right] \quad (18)$$

The above function  $f(z, z')$  is very useful for determining unsteady velocity, because the unsteady distribution of vortices  $\gamma_u$  has also the phase difference  $2\pi/N$  at the corresponding points on the blades.

Unsteady distribution of vortices  $\gamma_u$  consists of quasi-steady term  $\gamma_0$  and wake effect term  $\gamma_w$ ,

$$\gamma_u = \gamma_0 + \gamma_w \quad (19)$$

The induced velocity by  $\gamma_0$  has to cancel  $v_{Qn2}$ ,  $v_{\Gamma n2}$  and  $v_{\omega n2}$  of equation (9), (10) and (11) on each blade. This relation is expressed by a integral equation as

$$\int_{z_L}^{z_T} \gamma_0(z') \operatorname{Im}[f(z, z') e^{i\beta z/|z|}] dz' + v_{Qn2} + v_{\Gamma n2} + v_{\omega n2} = 0 \quad (20)$$

Introducing the Kutta's condition at the trailing edge,  $\gamma_0$  can be finally determined.

The free vortices  $\gamma_1$  are assumed to be carried downstream along the steady streamline starting from the trailing edge, which can be calculated by equation (17). All wake streamlines have the same geometry, but free vortices on them have also  $2\pi/N$  phase difference with one another. Considering the fact that the strength of free vortices is inversely proportional to the velocity, the distribution of free vortices  $\gamma_1$  of the reference blade can be written as

$$\gamma_1 = C \left| \frac{v(z_T)}{v(z)} \right| e^{j(\omega - \Omega)t} e^{-j h(s)} \quad (21)$$

Here,  $C$  is a complex constant with respect to  $j$ ,  $|v(z)|$  the absolute velocity on wake streamline,  $s$  the length of the streamline measured from the trailing edge  $z_T$ . The function  $h(s)$  in the above equation is defined further as

$$h(s) = (\omega - \Omega) \int_0^s ds' / |v(z')| \quad (22)$$

Assuming  $C=1$  provisionally, the velocities on the blade induced by free vortices,  $v_{wn}$  are written as

$$v_{wn}(z) = \operatorname{Im} \left[ \int_{z_T}^{\infty} \left| \frac{v(z_T)}{v(z')} \right| e^{-j h(s)} f(z, z') dz' e^{i\beta z/|z|} \right] \quad (23)$$

To cancel this normal component on the blade, the unsteady distribution of vortices  $\gamma_{w1}$  ( $\gamma_{w1} = \gamma_w / C$ ) is to satisfy the following integral equation

$$\int_{z_L}^{z_T} \gamma_{w1}(z') \operatorname{Im}[f(z, z') e^{i\beta z/|z|}] dz' + v_{wn}(z) = 0 \quad (24)$$

The above equation should be solved under the additional condition that the vortex strength is continuous at the trailing edge.

Introducing the circulations  $\Gamma_s$ ,  $\Gamma_0$  and  $\Gamma_{w1}$ , which are caused by  $\gamma_s$ ,  $\gamma_0$  and  $\gamma_{w1}$ , the total circulation  $\Gamma$  is

$$\Gamma = \Gamma_s + \Gamma_0 + C \Gamma_{w1} \quad (25)$$

Differentiating both sides of the equation (25) with respect to time and using  $d/dt = j(\omega - \Omega)$ ,

$$d\Gamma/dt = j(\omega - \Omega)(\Gamma_0 + C \Gamma_{w1}) \quad (26)$$

is obtained. Further, Kelvin's law for the conservation of vortices leads to the relation that the rate of total circulation change is equal to the total shed vortices from the trailing edge within unit time. This is expressed by

$$-d\Gamma/dt = C |v(z_T)| e^{-j h(0)} \quad (27)$$

where  $|v(z_T)|$  is the steady velocity at the trailing edge. Substitution of equation (27) into equation (26) yields,

$$C = \frac{-j(\omega - \Omega)\Gamma_0}{j(\omega - \Omega)\Gamma_{w1} + |v(z_T)|} \quad (28)$$

Once  $C$  is determined in the above, whole unsteady flow field can be solved completely.

#### Forces Acting on the Impeller

Forces acting on the impeller can be determined by integrating the pressure distribution on the blades. The assumption of infinitely thin blades makes this calculation comparatively simple. Let  $A$  and  $B$  be upper and lower surface of a blade point, the pressure difference between these points is expressed as

$$\begin{aligned} p_B/\rho - p_A/\rho &= (v_A^2 - v_B^2)/2 + \partial(\phi_A - \phi_B)/\partial t \\ &= (v_A + v_B) \gamma/2 + j(\omega - \Omega) \int_{z_L}^{z_A} (\gamma_0 + \gamma_w) dz \end{aligned} \quad (29)$$

where  $v_A$  and  $v_B$  are the local velocities, and  $\phi_A$  and  $\phi_B$  are the velocity potentials. Here  $(v_A + v_B)/2$ , the mean velocity of the both sides, is denoted by  $U_m$  and is separated further into steady component  $U_{m1}$  and unsteady component  $U_{m2}$ .  $U_{m1}$  can be obtained from equation (17),

$$U_{m1}(z_A) = v(z_A) \quad (30)$$

Now  $U_{m2}$  can be obtained by adding  $v_{Qt2}(z_A)$ ,  $v_{\Gamma t2}(z_A)$  and  $v_{\omega t2}(z_A)$  from equation (12), (13) and (14) to the tangential component of the velocities induced by  $\gamma_0$ ,  $\gamma_w$  and  $\gamma_1$ .

$$\begin{aligned}
U_{m2}(z_A) = & \left[ \int_{z_L}^{z_T} (\gamma_0(z') + \gamma_w(z')) \operatorname{Re} [f(z_A, z') e^{i\beta} z_A / |z_A|]_i dz' \right. \\
& + \int_{z_T}^{\infty} \gamma_1(z') \operatorname{Re} [f(z_A, z') e^{i\beta} z_A / |z_A|]_i dz' \left. \right] e^{j(\omega - \Omega)t} \Big]_j \cdot [z_A e^{i\beta} / |z_A|]_i \\
& + v_{Qt2}(z_A) + v_{\Gamma t2}(z_A) + v_{wt2}(z_A)
\end{aligned} \tag{31}$$

Consequently, the first term of the right side of equation (29) may be written as

$$\begin{aligned}
(v_A + v_B) \gamma / 2 &= (U_{m1} + U_{m2}) (\gamma_s + \gamma_0 + \gamma_w) \\
&\approx U_{m1} \gamma_s + U_{m1} (\gamma_0 + \gamma_w) + U_{m2} \gamma_s
\end{aligned} \tag{32}$$

where  $U_{m2}(\gamma_0 + \gamma_w)$ , which is second order quantities, is neglected. Integrating the pressure difference along all blades, and adding them up as vector quantities, the total force acting on the impeller is given as

$$\begin{aligned}
F = \rho \sum_{k=0}^{N-1} e^{-j2\pi k/N} e^{i2\pi k/N} \int_{z_L}^{z_T} [U_{m1}(z') [\gamma_0(z') + \gamma_w(z')] \\
+ U_{m2}(z') \gamma_s(z') + j(\omega - \Omega) \int_{z_L}^{z'} [\gamma_0(z) + \gamma_w(z)] dz]_j \cdot [iz' e^{i\beta} / |z'|]_i dz'
\end{aligned} \tag{33}$$

Obviously the total force obtained is purely oscillatory without any steady component. This is because steady component vanishes by adding up for all blades.

It is well known from thin airfoil theory that the direction of lift acting on an airfoil is perpendicular to the inlet flow direction, and the lift cannot be calculated by merely integrating the pressure difference between upper and lower surfaces along the airfoil. It is because the infinite strength of vortex at the leading edge generates a finite force in the chordwise direction. In this analysis,  $\gamma_s$  does not become infinite at the leading edge because shockless entry is assumed throughout. Even in this case,  $\gamma_0$  and  $\gamma_w$  become infinite at the leading edge. Calculation shows, however, that the effect remains always within second order quantities, and thus can be neglected. From the above considerations, it is evident that the integration of the pressure difference leads to the force acting on the impeller.



## Method of Numerical Calculation

In the practical calculation the vortex distribution on blades and wakes are replaced by finite number of discrete vortices, thus transforming the integral equations to simultaneous equations. In the calculation of unsteady vortices, it is noted that the coefficients of simultaneous equations become complex with respect to  $j$ . Numerical integrations should resort to trapezoidal method by separating the integrands into real and imaginary part. The integration of  $\gamma_1$  in equation (23) and (31) can be terminated at a proper distance from trailing edge, since the effect of free vortices diminishes rapidly as they get away from the impeller.

## Numerical Results

Calculations are carried out for blade angle  $\beta$  of  $30^\circ$ ,  $45^\circ$  and  $60^\circ$ . Some examples are given in figure 4,5 and 6. Figure 4 is the result for the case of  $N=6$ ,  $r_1/r_2=0.5$ ,  $\beta=45^\circ$ ,  $\Gamma_p=0$  and the flow coefficient  $\psi=0.25$ . The absolute values and the directions of dimensionless forces acting on the impeller at the moment when  $OO'$  is in the direction of  $x$  axis are shown for various values of  $\Omega/\omega$ . Though the forces acting on each blade are unsteady, the combined forces become always constant, provided the number of blades is greater than three. Observing from the relative coordinate system, the force changes its direction clockwise with the angular speed  $(\Omega-\omega)$ . While, observing from the fixed coordinate system, the direction changes clockwise with the angular speed  $\Omega$ . The angle between force vector and  $OO'$  remains constant. Figure 5 is the result for the case of  $N=6$ ,  $r_1/r_2=0.5$ ,  $\beta=30^\circ$ ,  $\Gamma_p=0$  and  $\psi=0.443$ , while figure 6 for the case of  $N=6$ ,  $r_1/r_2=0.5$ ,  $\beta=60^\circ$ ,  $\Gamma_p=0$  and  $\psi=0.1443$ .

In the stability analysis of a rotor system, hydrodynamic damping force acting on each element of the rotor plays a predominant role. In the present case damping force corresponds to the component of fluid force on the impeller, which is parallel and is in opposite direction to the whirling velocity of shaft center. When damping force is negative, that is, when the fluid force has such component that pushes the shaft center toward its whirling motion, there exists a danger that the rotor system runs into severe whirling.

In the results shown in figures 4, 5 and 6, damping force corresponds to the fluid forces in  $+y$  direction for  $\Omega>0$  and in  $-y$  direction for  $\Omega<0$ . As seen from figures, fluid force acts as damping throughout the calculated cases.

When  $\Omega$  is equal to  $\omega$  ( $\Omega/\omega=1$ ), flow through the impeller becomes steady and no free vortices shed out from the blades. In all other cases ( $\Omega/\omega\neq 1$ ), blades are always under unsteady condition and the influence of  $\partial\phi/\partial t$  term in equation (33) cannot be neglected. Quasi-steady treatment seems to be inappropriate especially for centrifugal impeller, because the wake vortices shed from one blade pass in the proximity of the next blade, thus resulting in a substantial interference. This tendency becomes more remarkable when blade angle is large.

Besides the examples shown in figures, calculations were performed for various combinations of parameters. From these results it becomes clear that the number of blades has little influence on the total forces.

## CONCLUDING REMARKS

Fluid forces on a centrifugal impeller, whose rotating axis whirls with a constant speed, was solved by the singularity method. Some typical examples of

results were shown in vector diagrams. Although the results of this paper are obtained for simplified geometries under idealized assumptions, they will suggest us the nature of fluid forces acting on whirling impeller.

The present study is expected to be extended to those cases in which the condition of shockless entry is eliminated and the effect of volute or guide vanes is taken into account. Experimental study is also under way by the authors and is expected to furnish data to be compared with the present analysis.

This study is supported by Scientific Research Fund of the Ministry of Education and by Hitachi, Ltd.

#### REFERENCE

1. Black, H.F., Effects of Hydraulic Forces in Annular Pressure Seals on the Vibrations of Centrifugal Pump Rotors, Journ. Mech. Eng. Science, Vol. 11, No. 2, 1969, pp. 206-213.
2. Black, H.F., Lateral Stability and Vibrations of High Speed Centrifugal Pump Rotors, Dynamics of Rotor, IUTAM Symposium, Lingby, Denmark, 1974, pp.56-74.
3. Chamieh, D. and Acosta, A.J., Dynamic Forces on a Whirling Centrifugal Rotor, Proc. 6th Conf. on Fluid Machinery, Vol. 1, Budapest, 1979, pp. 210-219.

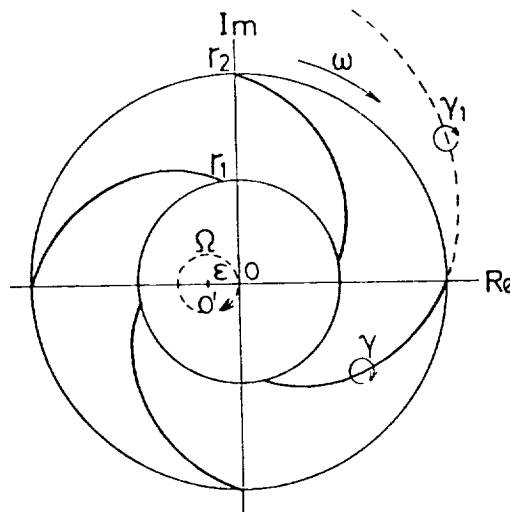


Fig. 1 Schematic geometry of a rotating impeller with whirling motion

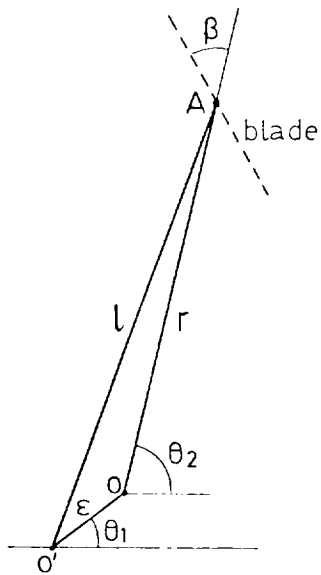


Fig. 2 Relation between center of impeller  $O$ , center of whirling  $O'$  and blade point  $A$

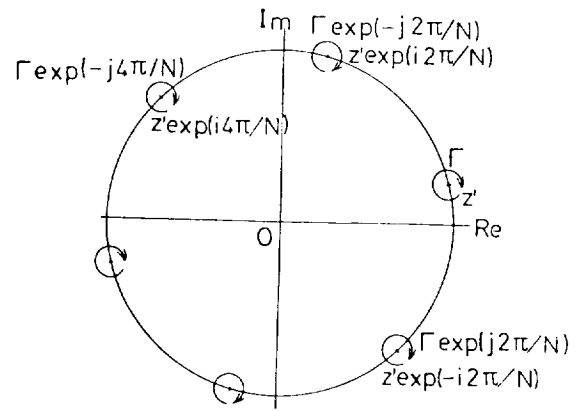


Fig. 3 Discrete vortices with phase difference  $2\pi/N$  ranged on a circumference with equal distance

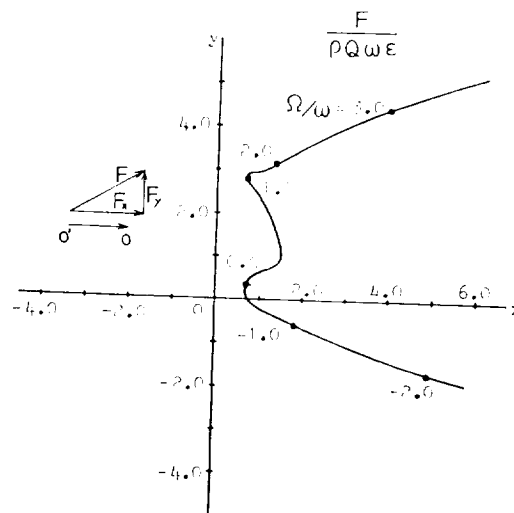


Fig. 4 Vector diagram of radial forces on whirling impeller ( $N=6$ ,  $\beta=45^\circ$ ,  $r_1/r_2=0.5$ ,  $\Gamma_p=0$ ,  $\psi=0.25$ )

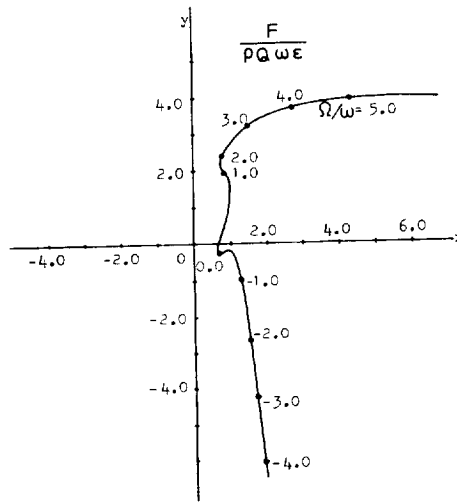


Fig. 5 Vector diagram of radial forces on whirling impeller ( $N=6$ ,  $\beta=30^\circ$ ,  $r_1/r_2=0.5$ ,  $\Gamma_p=0$ ,  $\psi=0.433$ )

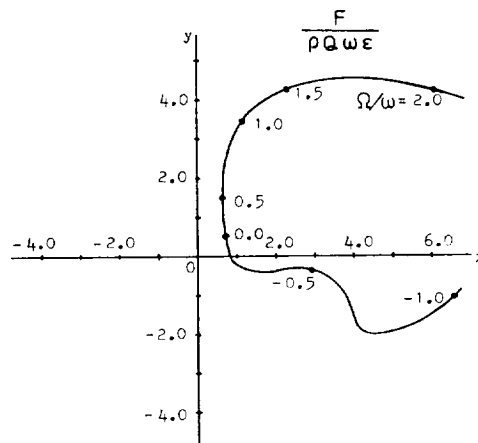


Fig. 6 Vector diagram of radial forces on whirling impeller ( $N=6$ ,  $\beta=60^\circ$ ,  $r_1/r_2=0.5$ ,  $\Gamma_p=0$ ,  $\psi=0.1443$ )